ADVANCED QUANTUM TECHNOLOGIES
www.advquantumtech.com

Higher-Order Spatially Squeezed Beam for Enhanced Spatial Measurements

Zhi Li, Hui Guo, Hongbo Liu, Jiaming Li, Hengxin Sun, Rongguo Yang, Kui Liu,* and Jiangrui Gao*

A scheme is proposed to realize high-precision spatial measurement of laser beams beyond quantum limit using a novel quantum state called the *m*th order spatially squeezed state, which is the combination of a bright $HG_{m,0}$ mode coherent state and squeezed vacuum $HG_{m+1,0}$ mode state. An effective technique for the generation of a rectangular shape higher-order mode squeezed light with a maximum mode order of 5 is experimentally demonstrated using a doubling resonated optical parametric amplifier. Furthermore, the fourth order tilt- and displacement-squeezed beams are constructed and used to perform spatial tilt and displacement measurements, thereby improving the signal-to-noise ratio by 10 and 8.6 dB compared to the $HG_{0,0}$ mode. The results indicate that high-order spatially squeezed states enhance measurement precision beyond the shot noise limit and are more prominent in back-action noise reduction. High-precision spatial measurement has potential practical applications in high-sensitivity atomic force microscope and super-resolution quantum imaging.

1. Introduction

High-precision spatial measurements of laser beams have found important applications in various areas, such as super-resolution imaging in optical microscope systems,[1,2] cantilever displacement in atomic-force microscopes,[3] biological, [4,5] and weak absorption measurements.[6,7] However, classical and quantum mechanical noise sources impose limitations on such measurements. Because of certain natural limits imposed by classical physics, the precision of a measurement can only achieve the shot noise limit (SNL) with statistical scaling of errors of the order $1/\sqrt{N}$. However, quantum technologies can offer enhanced measurement precision[8,9] beyond the SNL that outperforms the ultimate precision of the "Heisenberg limit" with a scaling of $1/N$. A fundamental problem is to find an effective quantum probe for spatial measurements with high precision.

Quantum metrology uses a nonclassical resource squeezed state to enhance the performance of measurements for various sensing applications.[3,10–12] For instance, the laser interferometer gravitational-wave observatory (LIGO) injects nonclassical squeezed light into a Michelson interferometer, thereby surpassing the SNL because of laser shot noise.[13,14] Various attributes of the squeezing state have been studied and observed to be promising for the corresponding measurements of quantities in quantum enhanced metrology.[15–17] Apart from LIGO, the squeezed state can also be applied to spatial measurements.[18–23] Recently, $HG_{1,0}$ squeezed modes have shown to significantly improve the observed nonclassical sensitivity for mode-matching deficiency losses.[24] Furthermore, this scheme can be extended to higher-order modes, thereby introducing higher enhancement factors in quantum metrology.[25,26] The thermal noise of high-order mode is smaller than that of the fundamental mode,[27,28] which effectively reduces the classical noise. Therefore, studying the advantages of the high-order mode and squeezed state to further improve the measurement precision is crucial.

In this study, an effective technique is developed for the generation of higher-order mode squeezed light. To our knowledge, a similar study was being pursued by Joscha Heinze et al.;[29] however, we used a doubling resonated optical parametric amplifier (OPA) to produce the high-order mode squeezed state that can decrease the pump power and enhance the pump's spatial mode purity to effectively obtain high-order spatial mode squeezing. The rectangular-shaped higher-order $HG_{m,0}$, ($m = 1$, 2, 3, 4, 5) with $HG_{5,0}$ mode squeezing of 4.3±0.15 dB was experimentally generated, which is the highest amount of squeezing reported for the $HG_{5,0}$ mode. Using the experimental results, a high-order spatially squeezed beam was constructed and used to

Z. Li, H. Guo, H. Liu, J. Li, H. Sun, R. Yang, K. Liu, J. Gao
State Key Laboratory of Quantum Optics and Quantum Optics Devices
Institute of Opto-Electronics
Shanxi University
Taiyuan 030006, China
E-mail: hxsun@sxu.edu.cn; liukui@sxu.edu.cn

Z. Li, H. Guo, H. Liu, J. Li, H. Sun, R. Yang, K. Liu, J. Gao
Collaborative Innovation Center of Extreme Optics
Shanxi University
Taiyuan 030006, China

The ORCID identification number(s) for the author(s) of this article can be found under https://doi.org/10.1002/qute.202200055

DOI: 10.1002/qute.202200055

demonstrate a displacement and tilt measurement beyond the SNL. A high-order tilt squeezed beam was experimentally generated up to the fourth order with 3.5 dB squeezing and a tilt precision of up to 13.7 prad $Hz^{-0.5}$, thereby improving the signal-to-noise ratio (SNR) up to 10 dB compared with $HG_{0,0}$. A displacement precision of 0.53 pm $Hz^{-0.5}$ corresponding to the fourth order displacement squeezed beam with 2 dB squeezing improved the SNR up to 8.6 dB compared with $HG_{0,0}$. Furthermore, the precision of displacements of cantilevers in atomic-force microscopes was simulated using a high-order spatially squeezed beam that facilitates measurement precision beyond the SNL and reduces back action noise. This study proposes a method for realizing high-precision spatial measurements that have applications in high-precision sensing, such as high-sensitivity atomic-force microscopes and super-resolution quantum imaging.

2. Theoretical Description

For a spatial measurement system, the positive frequency part of the probe beam's electric field operator can be written as follows[21]

$$\hat{\varepsilon}^{+}(x) = i\sqrt{\frac{\hbar\omega}{2\varepsilon_0 cT}}\sum_{n=0}^{\infty}\hat{a}_n u_n(x) \tag{1}$$

where, $\hbar$ is the reduced Planck's constant, ω is the frequency of the light field,ε_0 is the vacuum permittivity, c is the speed of light, T is the detection time, $u_n(x)$ is the transverse beam amplitude function of the Hermite Gauss modes, and $\hat{a}_n$ is the corresponding annihilation operator given as $\hat{a}_n = (\hat{X}_n + i\hat{Y}_n)/2$. $\hat{a}_n$ is usually expressed in the form of $\hat{a}_n = \langle\hat{a}_n\rangle + \delta\hat{a}_n$, where $\langle\hat{a}_n\rangle$ describes the coherent amplitude part and $\delta\hat{a}_n$ is the quantum noise operator.

The notation m in a bright $HG_{m,0}$ mode of the probe beam corresponds to the mth-order Hermite–Gaussian (HG) mode. Furthermore, $\langle\hat{a}_m\rangle = \sqrt{N}$, where N is the number of photons of the $HG_{m,0}$ mode and $\langle\hat{a}_n\rangle = 0$ for the other modes. The probe beam can be rewritten as follows

$$\hat{\varepsilon}^{+}(x) = i\sqrt{\frac{\hbar\omega}{2\varepsilon_0 cT}}\{\sqrt{N}u_m(x) + \sum_{n=0}^{\infty}\delta\hat{a}_n u_n(x)\} \tag{2}$$

For the case of a small displacement d and tilt θ, Taylor series is used to expand the displaced and tilted $HG_{m,0}$ field to the $HG_{m+1,0}$ field (here, the part of $HG_{m-1,0}$ field is not taken into account owing to the mode selection in the balanced homodyne detection).[25] Therefore, the probe beam can be written as follows

$$\hat{\varepsilon}^{+}_{d,\theta}(x) = i\sqrt{\frac{\hbar\omega}{2\varepsilon_0 cT}}\{\sqrt{N}[u_m(x) + \frac{d}{\omega_0}[\sqrt{m+1}\cdot u_{m+1}(x)] + i\frac{\omega_0\pi\theta}{\lambda}[\sqrt{m+1}\cdot u_{m+1}(x)]] + \sum_{n=0}^{\infty}\delta\hat{a}_n u_n(x)\} \tag{3}$$

The parameters d and θ of a $HG_{m,0}$ beam are projected onto $u_{m+1}(x)$. The amplitude $\hat{X}_{m+1}$ and phase $\hat{Y}_{m+1}$ operators of the $u_{m+1}(x)$ mode are related to the displaced and tilted $HG_{m,0}$ mode.

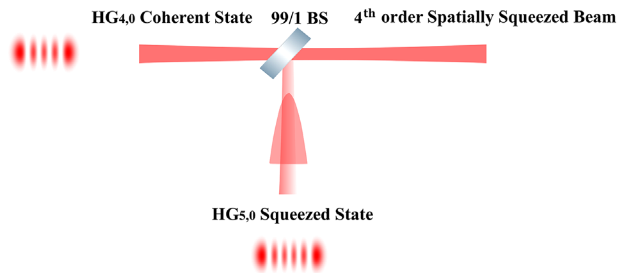

Figure 1. Higher-order spatially squeezed beam.

Therefore, the definitions of $HG_{m,0}$ mode displacement $\hat{d}_m$ and tilt $\hat{\theta}_m$ operators can be extended as follows

$$\hat{d}_m = \frac{\omega_0}{2\sqrt{N}\sqrt{m+1}}\hat{X}_{m+1} \tag{4}$$

$$\hat{\theta}_m = \frac{\lambda}{2\pi\sqrt{N}\omega_0\sqrt{m+1}}\hat{Y}_{m+1} \tag{5}$$

At $m = 0$, Equations (4) and (5) correspond to d and θ for the $HG_{0,0}$ mode.[18]

The fluctuations in the displacement and tilt operators of the $HG_{m,0}$ mode are given by $\delta\hat{d}_m = \omega_0 \cdot \delta\hat{X}_{m+1}/(2\sqrt{N}\sqrt{m+1})$ and $\delta\hat{\theta}_m = \lambda \cdot \delta\hat{Y}_{m+1}/(2\pi\sqrt{N}\omega_0\sqrt{m+1})$, where are related to the fluctuation of the amplitude and phase operators of the $HG_{m+1,0}$ mode. When the $HG_{m+1,0}$ mode is a vacuum state ($\delta\hat{X}_{m+1} = 1$ and $\delta\hat{Y}_{m+1} = 1$), it corresponds to the SNL for the fluctuation of displacement and tilt operators. When the vacuum $HG_{m+1,0}$ mode is squeezed in amplitude or phase quadrature ($\delta\hat{X}_{m+1} = e^{-r} < 1$ or $\delta\hat{Y}_{m+1} = e^{-r} < 1$), the fluctuation of displacement or tilt operator is below the SNL. Here, r is the factor associated with squeezing. With an increase in both the squeezing degree and mode order, the fluctuation decreases. If the high-order spatially squeezed beam is used as the probe beam, the quantum noise should be squeezed more effectively in the measurement of displacement and tilt beyond the SNL ($\delta\hat{d}_m = \omega_0 \cdot e^{-r}/(2\sqrt{N}\sqrt{m+1})$ and $\delta\hat{\theta}_m = \lambda \cdot e^{-r}/(2\pi\sqrt{N}\omega_0\sqrt{m+1})$).

Therefore, the new state is defined as the combination of a bright $HG_{m,0}$ mode coherent state and a squeezed vacuum $HG_{m+1,0}$ mode state for the mth order spatially squeezed beam (SSB). For instance, a fourth order SSB is constructed by mixing the squeezed vacuum $HG_{5,0}$ mode state with the bright $HG_{4,0}$ mode coherent state using a 99/1 beam splitter, as shown in **Figure 1**. Here, the vacuum $HG_{5,0}$ mode is squeezed in amplitude quadrature ($\delta\hat{X}_5 < 1$), called the fourth order displacement squeezed beam (DSB). In contrast, the vacuum $HG_{5,0}$ mode is squeezed in the phase quadrature ($\delta\hat{Y}_5 < 1$), which is the fourth order tilt squeezed beam (TSB).

3. Experimental Setup and Results

3.1. The Experimental Setup Used for the Generation of a Higher-Order Spatially Squeezed Beam

To construct a high-order spatially squeezed state, a high-quality high-order mode squeezed state must be primarily generated

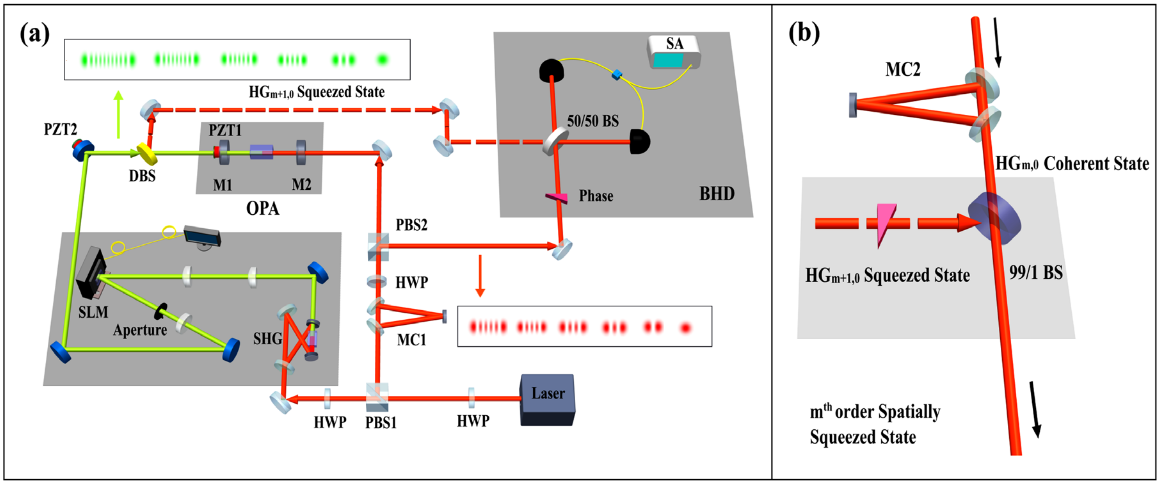

Figure 2. Schematic of the experimental setup. Optical parametric amplifier (OPA), second harmonic generation (SHG), dichroic beam splitter (DBS), mode convert cavity (MC), polarizing beam splitter (PBS), beam splitter (BS), spatial light modulator (SLM), half-wave plate (HWP), piezoelectric element for controlling phases (PZT), balance homodyne detection (BHD), spectrum analyzer (SA).

using the following two methods: i) transforming the fundamental mode squeezed state into the high-order mode squeezed state using a mode conversion system,[30–32] which is limited by system losses; ii) directly generating the high-order mode squeezed state using an OPA operating at a high-order mode. To generate the perfect high-order mode squeezed state, an effective technique was developed to experimentally demonstrate a high-quality first to fifth order squeezed state.

In general, the OPA operated at fundamental modes for the pump and down conversion beams. Pumping at the fundamental mode made it possible to obtain a squeezed state for the first few order space modes, for instance, $HG_{0,1}$ and $HG_{0,2}$. In the fundamental pump, the fundamental down conversion mode oscillated more easily compared to the high-order mode. When the OPA oscillated at the fundamental mode, the pump power in the cavity was locked at the fundamental mode threshold power whose value was much smaller than that for the high-order mode. It was difficult to obtain a well-squeezed state because the OPA operated above the threshold,[33–36] as previously demonstrated for the generation of $HG_{1,0}$ mode.[37]

To generate a high-quality first to fifth order squeezed state, obtaining a spatially matched pump mode was crucial to improve the nonlinear conversion efficiency. Theoretical analysis indicated that the $HG_{m,0}$ squeezed states corresponding to the optimal spatially matched superposition modes are $HG_{0,0}$, $\dots .HG_{2m-2,0}$, $HG_{2m,0}$.[33,37] The optimal superposition and signal modes cannot resonate simultaneously in the degenerate DOPA cavity. Therefore, the optimal single spatially matched pump mode $HG_{2m,0}$ is experimentally demonstrated to generate the $HG_{m,0}$ squeezed state.

For the signal mode $HG_{m,0}$, the threshold of the optimal single pump mode $HG_{2m,0}$ increased with the mode order m using the same OPA cavity. For instance, assuming that the signal mode resonant in the OPA was a $HG_{0,0}$ mode, the threshold for the pump mode $HG_{0,0}$ was 200 mW. For a $HG_{5,0}$ signal mode, the threshold for the pump mode $HG_{10,0}$ increased to ≈800 mW. As the mode order increased, the Watts of magnitude optimal pump mode $HG_{2m,0}$ were required to operate in the OPA for a single resonant cavity. It was difficult to experimentally produce a high-power high-order pump mode $HG_{2m,0}$. Therefore, a doubling resonant OPA cavity with a buildup factor of ≈70 for the pump light was designed, which can lower the threshold of the high-order mode. In addition to the optimal single pump mode, the external cavity pump field included other spatial modes mismatched with the signal mode; thereby reducing the coupling efficiency of the pump mode and introducing other losses into the OPA cavity. In the experiment, a doubling resonant OPA cavity was used to generate the $HG_{m,0}$ squeezed state, which was more prominent in the purity of the spatial mode of pump compared to the single resonance OPA cavity.

The OPA cavity consisted of two plano-concave mirrors with a radius of curvature of 30 mm (M1 and M2 in **Figure 2**a) and a $1 \times 2 \times 10$ mm^3 periodically poled potassium titanyl phosphate (PPKTP) crystal in the center. The cavity was nearly concentric with a length of 62.3 mm and had a waist of 43 μm in the infrared and 30 μm in the green for $HG_{0,0}$. Cavity mirror M1 was $T =$ 10% at 1080 nm and T = 5% at 540 nm, and cavity mirror M2 was highly reflective ($R >$ 99.95%) at both 1080 and 540 nm. The PPKTP crystal temperature can be fine-tuned to achieve phase-matching and a doubly resonant pump-signal mode.

Figure 2a shows the experimental setup used for the generation of a high-order mode squeezed state. Continuous-wave light beam at 1080 nm from a fiber laser was split into two. One of the beams remained in the $HG_{0,0}$ mode and was upconverted to 540 nm using cavity-enhanced second harmonic generation. Furthermore, two cylindrical lenses were used to shape the $HG_{0,0}$ mode into an elliptical spot that was converted into the $HG_{2m,0}$ mode using a spatial light modulator. The elliptical spot could improve the conversion efficiency of the $HG_{2m,0}$ mode. The spatial distribution of the $HG_{2m,0}$ mode was more comparable with the elliptical spot than the $HG_{0,0}$ mode.[38] The $HG_{2m,0}$ mode was used for the pump mode to operate an OPA for generating the $HG_{m,0}$ squeezed light, which was separated from the $HG_{2m,0}$ pump mode using a dichroic beam splitter. The other beam passed through the mode converter MC1 that converted the $HG_{0,0}$ mode into a standard $HG_{m,0}$ mode (m = 0,1,2,3,4,5). A

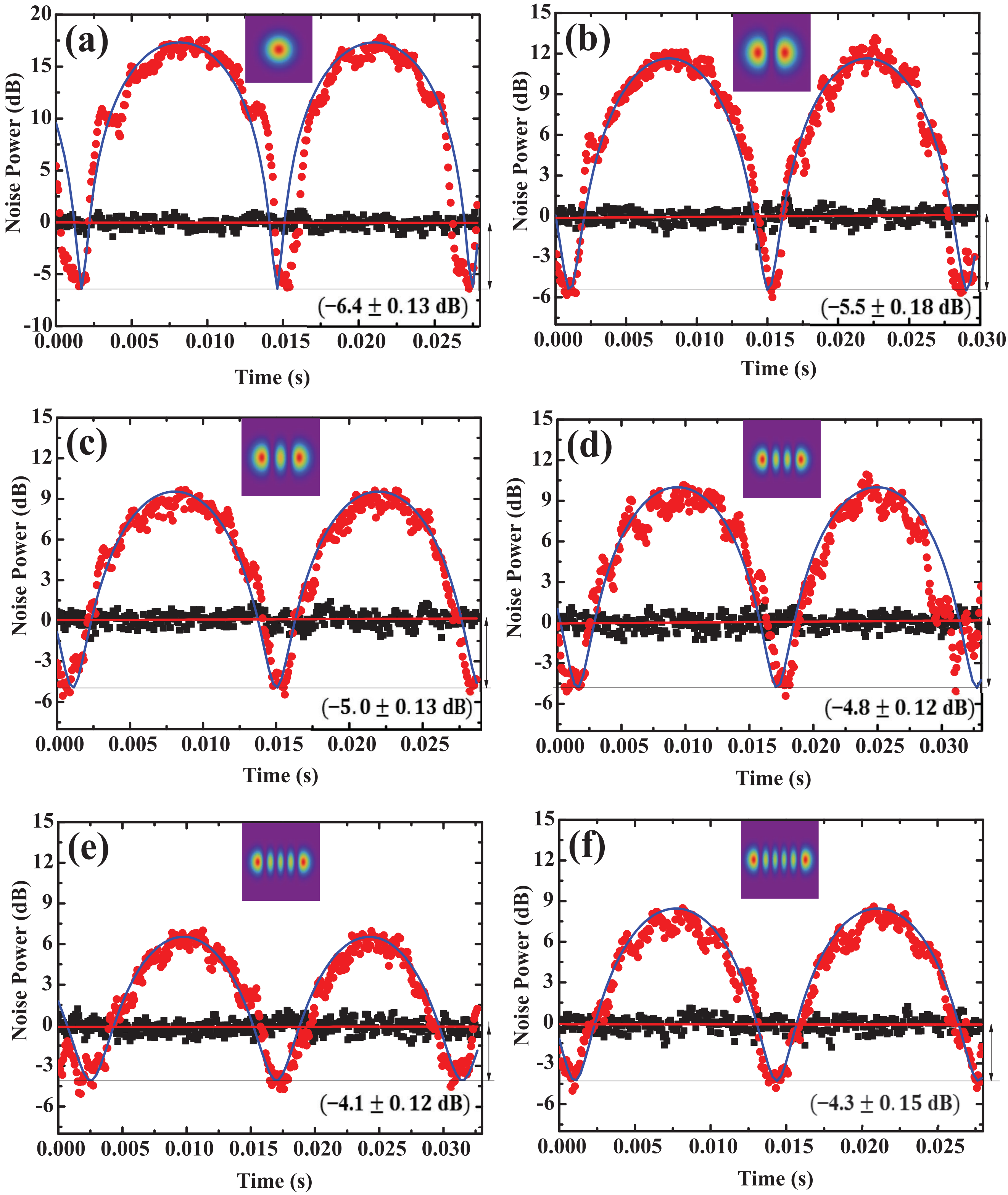

Figure 3. Experimental results for high-order Hermite–Gaussian squeezed light. Trace (i) (black line): SNL. Trace (ii) (red line) corresponds to quantum noise levels of the generated mode squeezed state with scanning of the local beam phase. The measurement parameters for the spectrum analyzer are RBW, 300 kHz; VBW, 470 Hz; and analysis frequency, 3 MHz.

fraction of the $HG_{m,0}$ mode was used as the seed beam. The relative phase between the pump field and injected seed beam was locked in a state of deamplification using PZT2 for generating an amplitude quadrature squeezed light. The remaining part of the $HG_{m,0}$ mode was used as a local oscillator for balanced homodyne detection (BHD).

Figure 3 shows the generated squeezing. The high-order mode squeezed light from $HG_{0,0}$ to $HG_{5,0}$ was directly generated using the doubling resonated OPA cavity. The corresponding power of the pump mode for $HG_{0,0}$, $HG_{2,0}$, $HG_{4,0}$, $HG_{6,0}$, $HG_{8,0}$, $HG_{10,0}$ is ≈40, 50, 60, 80, 50, and 60 mW, respectively. As shown in Figure 3a, the $HG_{0,0}$ mode squeezing level is −6.4±0.13 dB, limited by the cavity losses and measurement efficiency. The squeezing from $HG_{1,0}$ to $HG_{5,0}$ at 3 MHz (Figure 3b–f) is −5.5±0.18, −5.0±0.13, −4.8±0.12, −4.1±0.12, and −4.3±0.15 dB, respectively. The squeezing level for the $HG_{m,0}$ ($m = 1, 2, 3, 4, 5$) mode decreases compared to the $HG_{0,0}$ mode because the damage threshold for the spatial light modulator limits the pump power of the $HG_{2m,0}$ mode. For instance, as shown in Figure 3e, the squeezing level of the $HG_{4,0}$ mode is −4.1±0.12 dB that was limited by the pump power of the $HG_{8,0}$ mode (just 50 mW). The threshold of the $HG_{0,0}$ signal mode is ≈60 mW and that of the $HG_{5,0}$ signal mode for theoretical calculation is 244 mW; however, the former might be less than 60 mW because the optimal phase-matching condition could not be achieved by tuning the temperature of PPKTP crystals. In future studies, the crystal temperature and cavity length can be simultaneously fine-tuned to achieve the optimal doubly resonant phase-matching condition that may reduce the current pump threshold.

As the mode order increases, the squeezing level is degraded by inefficiencies in the measurement process. The transmission efficiency is 0.98±0.01, and the quantum efficiency of the detector is 0.97±0.01. The interference visibility of the squeezed light $HG_{5,0}$, $HG_{4,0}$, $HG_{3,0}$, $HG_{2,0}$, $HG_{1,0}$, $HG_{0,0}$ is 0.96±0.02, 0.97±0.02, 0.97±0.02, 0.98±0.01, 0.98±0.01 and 0.99±0.005, respectively. The visibility is inversely proportional to the mode order because the high-order mode has a complex distribution that is more sensitive compared to the fundamental mode $HG_{0,0}$.[39] The interference visibility greater than 95% implies that the mode purity of generated squeezing state is almost ideal.

As shown in Figure 2b, the $HG_{m+1,0}$ squeezed light was coupled with the bright coherent light in the $HG_{m,0}$ mode on a 99:1 beam splitter to construct the mth order spatially squeezed beam. The infrared light passed through the mode converter MC2, which converted the $HG_{0,0}$ mode into the standard $HG_{m,0}$ mode as a bright coherent beam. The relative phase between the $HG_{m+1,0}$ squeezed light and $HG_{m,0}$ coherent light is locked to 0 or $\pi/2$ to generate the mth order displacement or tilt squeezed beam.

Figure 4 shows the relative power spectrum with the tilt fluctuation for different probe beams, such as the $HG_{0,0}$ (Trace (i)), $HG_{4,0}$ (Trace (ii)) and the fourth order TSB (Trace (iii)). Compared with the $HG_{0,0}$ mode, the tilt fluctuation of the $HG_{4,0}$ mode is reduced by 6.5±0.13 dB and that of the $HG_{m,0}$ mode is inversely proportional to the mode order m. Compared with the $HG_{4,0}$ mode, the $HG_{5,0}$ squeezed light reduces the tilt fluctuation of fourth order TSB by 3.5±0.15 dB, which is lower than the SNL noise for $HG_{0,0}$ at 10±0.12 dB implying that the tilt noise is "squeezed." In Figure 4, a distinct peak centered at a frequency of 3 MHz corresponding to the mean of the tilt is observed. The fourth order TSB is slightly lower than the squeezing of the $HG_{5,0}$ mode because of the losses at the beam splitter and mode matching. The squeezing levels from the fundamental to third order TSB at 3 MHz are 3.2±0.13, 3.8±0.18, 3.2±0.13 and 3.3±0.12 dB, respectively.

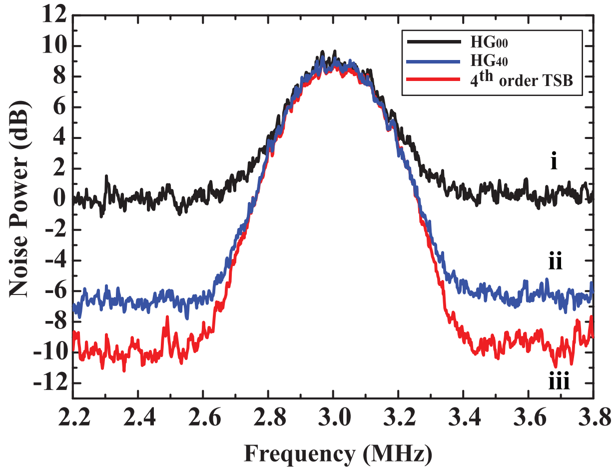

Figure 4. The spatial fluctuation noise for i) $HG_{0,0}$, ii) $HG_{4,0}$, and iii) fourth order tilt squeezed beam as the probe beam. The spectrum analyzer settings were as follows: RBW, 300 kHz; VBW, 470 Hz.

3.2. Higher-Order Spatially Squeezed Beam for Enhanced Spatial Measurements

The mth order spatially squeezed beam, that is, the probe beam, is passed through a wedged crystal that simulates a slight tilt signal, as shown in **Figure 5**b. This signal can be transformed into a slight displacement by applying Fourier transformation using a lens.[40] The modulated probe beam and 1 mW local beam $HG_{m+1,0}$ are coupled using a 50/50 beam splitter and detected using BHD. The difference photocurrent of BHD was analyzed using an electrical spectrum analyzer to demodulate the displacement or tilt signals.

The square root of signal-to-noise ratios of various probe beams corresponding to the amplitude of the tilt signal are shown in **Figure 6**a at 3 MHz. The $\sqrt{\mathrm{SNR}}$ of the fourth order TSB (Trace (iii)) increased faster than that of $HG_{0,0}$ (Trace (i)). At $\sqrt{\mathrm{SNR}}=1$, minimum precisions of 43.5 prad Hz$^{-0.5}$, 29.5 prad Hz$^{-0.5}$ and 13.7 prad Hz$^{-0.5}$ were obtained for the $HG_{0,0}$ coherent probe beam, fundamental mode TSB, and fourth order TSB, respectively. Thus, improvement by a factor of 3.2 was achieved over the shot noise limited between the $HG_{0,0}$ coherent and fourth order TSBs, and the corresponding SNR increased by 10 dB. As the probe beam was in the fourth order TSB, the measurement noise level was below the shot noise limit of 3.5±0.15 dB. The probe beam power was 25 μW, and the beam waist size of $HG_{0,0}$ is 350 μm. The displacement measurement is shown in Figure 6b. The minimum precision for the displacement obtained with the $HG_{0,0}$ coherent beam was 1.44 pm Hz$^{-0.5}$, corresponding to the fundamental mode and fourth order DSBs with values of 1.02 and 0.53 pm Hz$^{-0.5}$, respectively. An improve-

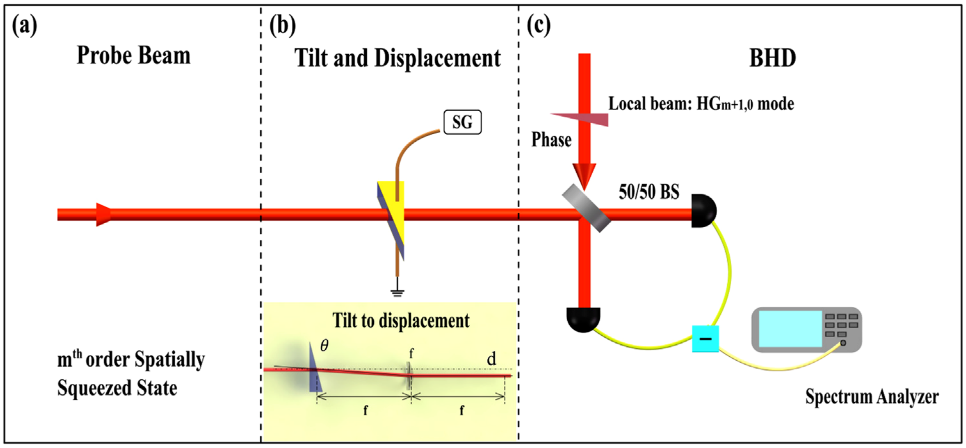

Figure 5. The experimental setup used for measuring the displacement and tilt by a high-order spatially squeezed beam. Signal generator (SG), beam splitter (BS), balanced homodyne detection (BHD).

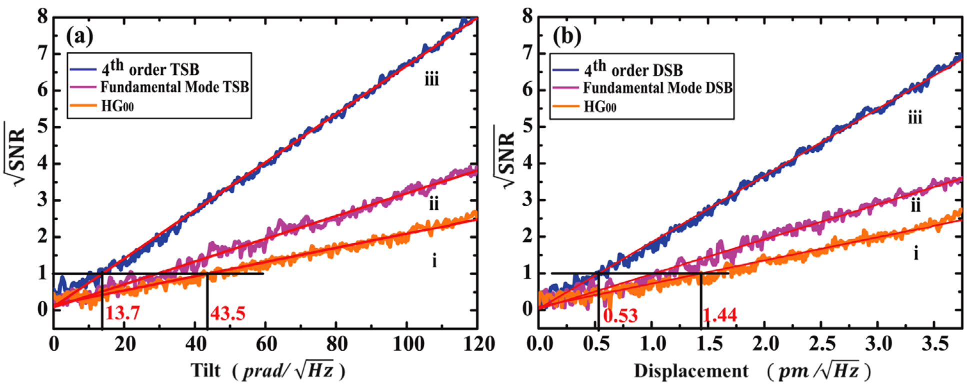

Figure 6. a) The square root of signal-to-noise ratio ($\sqrt{\text{SNR}}$) versus linearly increasing tilt amplitude for i) the coherent beam $HG_{0,0}$, ii) fundamental mode TSB, iii) and fourth order TSB. b) The square root of signal-to-noise ratio versus linearly increasing displacement amplitude for i) coherent beam $HG_{0,0}$, ii) fundamental mode DSB, and iii) fourth order DSB.

ment by a factor of 2.7 was achieved over the shot noise limited between the $HG_{0,0}$ coherent beam and the fourth order DSB, and the corresponding SNR increased by 8.6 dB. The noise level of the fourth order DSB was reduced to 2±0.1 dB. The probe beam power was 60 μW, and the beam waist size of $HG_{0,0}$ was 50 μm. The minimum precision was degraded by inefficiency in the measurement process. Here, the total detection efficiency for the $HG_{0,0}$ coherent probe beam, fundamental mode, and fourth order TSB is 0.93±0.02, 0.90±0.02, and 0.83±0.02, respectively. The measurement efficiency of the photodiode was 0.97±0.01, the spatial overlap efficiency between the signal beam and local beam was 0.98±0.01, and the spatial overlap efficiency between the signal beam and squeezed beam for $HG_{1,0}$ and $HG_{5,0}$ was 0.98±0.01 and 0.96±0.02, respectively. The transmission efficiency was 0.97±0.02. The measurement parameters for the spectrum analyzer were RBW, 300 kHz and VBW, 470 Hz.

The minimum precision of the tilt signal corresponded to the mode order for coherent and spatially squeezed beams that displayed a quantum noise reduction of 3.0±0.1 dB, as shown in **Figure 7**. The minimum precision improved with increasing mode order for the coherent and squeezed states, which corresponded to the theoretical prediction.

The high-order spatially squeezed beam will be an accessible and stable probe beam for the application of optical sensors. The cantilever displacement in an atomic-force microscope was theoretically simulated in ref. [3]; the microcantilever showed a fundamental resonance at 13 kHz, a force constant of 0.2 N m^{-1} and a quality factor of 124. The displacement noise versus optical power of the different probe beams, $HG_{0,0}$ corresponding to the SNL (Trace (i)), 3.5 dB fundamental mode SSB (Trace (ii)), 3.5 dB fourth order SSB (Trace (iii)), and 3.5 dB tenth order SSB (Trace (iv)), are shown in **Figure 8** at a wavelength of 1080 nm. The minimum precision of the $HG_{0,0}$, fundamental mode SSB, fourth order SSB and tenth order SSB was d_A = 0.76 fm Hz$^{-0.5}$, d_B = 0.63 fm Hz$^{-0.5}$, d_C = 0.44 fm Hz$^{-0.5}$, d_D = 0.38 fm Hz$^{-0.5}$, respectively, at a probe beam power of 5 mW. The results indicated that high-order spatially squeezed states enhanced measurement precision beyond the shot noise limit and were more prominent in back-action noise reduction.

4. Conclusion

In this study, a new quantum state called the high-order spatially squeezed state was proposed, which has lower spatial fluctua-

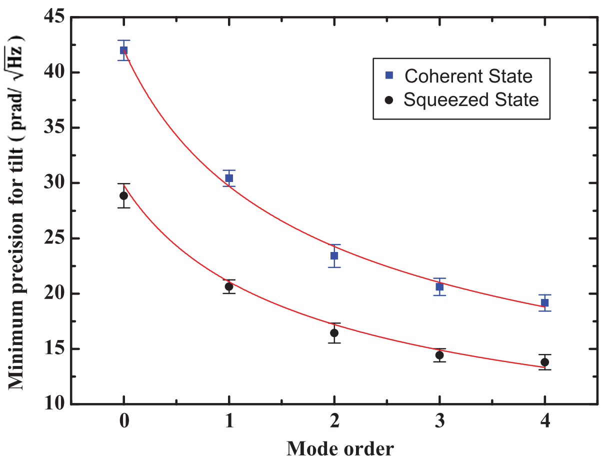

Figure 7. The minimum precision for the tilt obtained using a $HG_{0,0}$ (0-order), $HG_{1,0}$ (1-order), $HG_{2,0}$ (2-order), $HG_{3,0}$ (3-order), $HG_{4,0}$ (4-order) coherent beam (square dot), and the corresponding- order tilt squeezed beam (circle dot). The red line shows the theoretical fitting curve.

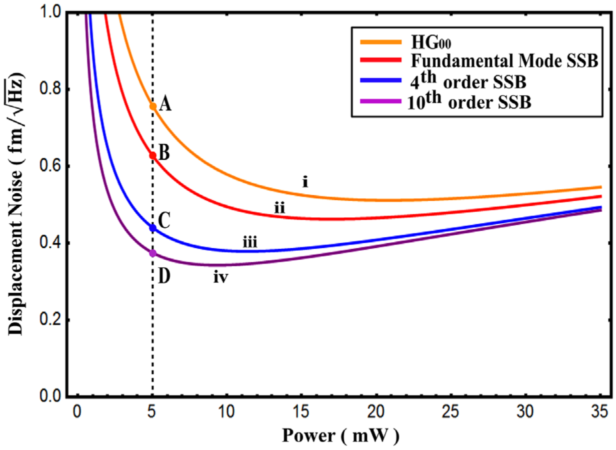

Figure 8. The theoretical calculations the displacement noise for a gold-coated microcantilever. The curves show the displacement noise versus optical power of the probe beam, the probe beam including i) $HG_{0,0}$, ii) 3.5 dB fundamental mode SSB, iii) 3.5 dB fourth order SSB, iv) 3.5 dB tenth order SSB.

tion. A high-precision measurement of the displacement and tilt using the high-order spatially squeezed state was experimentally demonstrated, which resulted in a larger enhancement over the $HG_{0,0}$ mode and precision beyond the SNL. The spatial measurement method has potential practical applications in super-resolution imaging in optical microscope systems, displacements of cantilevers in atomic-force microscopes, biological measurements, and weak absorption measurements. The cantilever displacement in an atomic-force microscope was theoretically simulated, and the high-order spatially squeezed beam was demonstrated to enhance measurement precision beyond the SNL and observed to be more prominent in back action noise reduction.

The experimental condition considered in this study was that the photon number N of the probe beam is much larger than the mode order $m(N \gg m)$, thereby resulting in a precision beyond the SNL. Whether the measurement precision may attain or surpass the Heisenberg limit at $N = m$ is an open research problem.

A recent study has shown that super-resolution imaging can be achieved based on spatial mode sorting or heterodyne detection using an HG local oscillator mode with a classical illumination beam.[41] Combining super-resolution schemes and high-order spatial squeezing, super-resolution imaging beyond the quantum limit can be explored.

An effective technique for the generation of higher-order squeezed light was developed. Using the setup employed in this study, the rectangular shape higher-order $HG_{m,0}$ mode ($m = 1$, 2, 3, 4, 5) and $HG_{5,0}$ mode squeezing at 4.3 ± 0.15 dB were generated, which correspond to the highest amount of squeezing reported thus far in the $HG_{5,0}$ mode. The squeezing was limited by the pump power and intracavity loss of the setup. Using advanced techniques, it may be possible to obtain squeezing greater than 10 dB, which will be promising for vastly improving the sensitivity of spatial measurements. The proposed technique can be expanded to other types of spatial modes to realize extremely specific tasks, such as $HG_{m,m}$ and $LG_{m,m}$ mode squeezing for an advanced LIGO.[28,42]

Acknowledgements

This work is supported by the National Natural Science Foundation of China (Grants Nos. 91536222, 12074233, and 11874248), Shanxi (1331 Project) and Shanxi Scholarship Council of China (2021-05).

Conflict of Interest

The authors declare no conflict of interest.

Data Availability Statement

The data that support the findings of this study are available from the corresponding author upon reasonable request.

Keywords

higher-order spatially squeezed beam, optical parametric amplifier, spatial measurement

Received: June 16, 2022
Revised: August 8, 2022
Published online: September 6, 2022

[1] E. Betzig, G. Patterson, R. Sougrat, W. Lindwasser, S. Olenych, J. Bonifacino, M. Davidson, J. Lippincott-Schwartz, H. Hess, *Science* **2006**, *313*, 1642.
[2] F. Yang, A. Taschilina, E. Moiseev, C. Simon, A. Lvovsky, *Optica* **2016**, *3*, 1148.
[3] R. C. Pooser, B. J. Lawrie, *Optica* **2015**, *2*, 393.
[4] M. Taylor, J. Janousek, V. Daria, J. Knittel, B. Hage, H.-A. Bachor, W. Bowen, *Phys. Rev. X* **2013**, *4*, 011017.
[5] M. Taylor, J. Janousek, V. Daria, J. Knittel, B. Hage, H.-A. Bachor, W. Bowen, *Nat. Photonics* **2012**, *7*, 229.

[6] A. C. Boccara, D. Fournier, J. Badoz, *Appl. Phys. Lett.* **1980**, *36*, 130.
[7] W. Dickmann, J. Dickmann, F. Bruns, S. Kroker, *Appl. Phys.Lett.* **2019**, *126*, 025106.
[8] V. Giovannetti, S. Lloyd, L. Maccone, *Nat. Photonics* **2011**, *5*, 222.
[9] V. Giovannetti, S. Lloyd, L. Maccone, *Phys. Rev. Lett.* **2006**, *96*, 010401.
[10] R. C. Pooser, N. Savino, E. Batson, J. L. Beckey, J. Garcia, B. J. Lawrie, *Phys. Rev. Lett.* **2020**, *124*, 230504.
[11] G. Triginer Garces, H. M. Chrzanowski, S. Daryanoosh, V. Thiel, A. L. Marchant, R. B. Patel, P. C. Humphreys, A. Datta, I. A. Walmsley, *Appl. Phys. Lett.* **2020**, *117*, 024002.
[12] R. B. de Andrade, H. Kerdoncuff, K. Berg-Sørensen, T. Gehring, M. Lassen, U. L. Andersen, *Optica* **2020**, *7*, 470.
[13] R. Schnabel, N. Mavalvala, D. McClelland, P. K. Lam, *Nat. Commun.* **2010**, *1*, 121.
[14] S. Pirandola, B. Bardhan, T. Gehring, C. Weedbrook, S. Lloyd, *Nat. Photonics* **2018**, *12*, 724.
[15] U. Andersen, T. Gehring, C. Marquardt, G. Leuchs, *Phys. Scr.* **2016**, *91*, 053001.
[16] F. Wolfgramm, A. Cere, F. Beduini, A. Predojevic, M. Koschorreck, M. Mitchell, *Phys. Rev. Lett.* **2010**, *105*, 053601.
[17] B. Lamine, C. Fabre, N. Treps, *Phys. Rev. Lett.* **2008**, *101*, 123601.
[18] M. Hsu, W. Bowen, N. Treps, P. K. Lam, *Phys. Rev. A* **2005**, *72*, 013802.
[19] C. Fabre, J. Fouet, A. Maitre, *Opt. Lett.* **2000**, *25*, 76.
[20] N. Treps, N. Grosse, W. Bowen, C. Fabre, H.-A. Bachor, P. K. Lam, *Science* **2003**, *301*, 940.
[21] V. Delaubert, N. Treps, M. Lassen, C. C. Harb, C. Fabre, P. K. Lam, H.-A. Bachor, *Phys. Rev. A* **2006**, *74*, 053823.
[22] N. Treps, U. Andersen, B. Buchler, P. K. Lam, A. Maitre, H.-A. Bachor, C. Fabre, *Phys. Rev. Lett.* **2002**, *88*, 203601.
[23] K. Liu, C. Cai, J. Li, L. Ma, H. Sun, J. Gao, *Appl. Phys. Lett.* **2018**, *113*, 261103.
[24] S. Steinlechner, N.-O. Rohweder, M. Korobko, D. Toyra, A. Freise, R. Schnabel, *Phys. Rev. Lett.* **2018**, *121*, 263602.
[25] H. Sun, K. Liu, Z. Liu, P. Guo, J. Zhang, J. Gao, *Appl. Phys. Lett.* **2014**, *104*, 121908.
[26] B. Xia, J. Huang, C. Fang, H. Li, G. Zeng, *Phys. Rev. Appl.* **2020**, *13*, 034023.
[27] S. Chelkowski, S. Hild, A. Freise, *Phys. Rev. D* **2009**, *79*, 122002.
[28] L. Tao, A. Green, P. Fulda, *Phys. Rev. D* **2020**, *102*, 122002.
[29] J. Heinze, B. Willke, H. Vahlbruch, *Phys. Rev. Lett.* **2022**, *128*, 083606.
[30] L. Ma, H. Guo, H. Sun, K. Liu, B. Su, J. Gao, *Photonics Res.* **2020**, *8*, 1422.
[31] J.-F. Morizur, S. Armstrong, N. Treps, J. Janousek, H.-A. Bachor, *Eur. Phys. J. D* **2011**, *61*, 237.
[32] M. Semmler, S. Berg-Johansen, V. Chille, C. Gabriel, P. Banzer, A. Aiello, C. Marquardt, G. Leuchs, *Opt. Express* **2016**, *24*, 7633.
[33] M. Lassen, V. Delaubert, C. Harb, P. K. Lam, N. Treps, H.-A. Bachor, *J. Eur. Opt. Soc. Rapid Publ.* **2006**, *1*, 06003.
[34] M. Lassen, V. Delaubert, J. Janousek, K. Wagner, H.-A. Bachor, P. K. Lam, N. Treps, P. Buchhave, C. Fabre, C. Harb, *Phys. Rev. Lett.* **2007**, *98*, 083602.
[35] M. Lassen, G. Leuchs, U. Andersen, *Phys. Rev. Lett.* **2009**, *102*, 163602.
[36] K. Liu, J. Guo, C. Cai, S. Guo, J. Gao, *Phys. Rev. Lett.* **2014**, *113*, 170501.
[37] J. Guo, C. Cai, L. Ma, K. Liu, H. Sun, J. Gao, *Opt. Express* **2017**, *25*, 4985.
[38] K. Liu, Z. Li, H. Guo, J. Gao, *Chin. J. Lasers* **2020**, *47*, 6.
[39] J. Heinze, H. Vahlbruch, B. Willke, *Opt. Express* **2020**, *45*, 5262.
[40] H. Sun, Z. Li, H. Guo, K. Liu, J. Gao, *Rev. Sci. Instrum.* **2021**, *92*, 064504.
[41] M. Tsang, R. Nair, X.-M. Lu, *Phys. Rev. X* **2016**, *6*, 031033.
[42] P. Fulda, K. Kokeyama, S. Chelkowski, A. Freise, *Phys. Rev. D* **2010**, *82*, 012002.